Redox Biology 47 (2021) 102167

Contents lists available at ScienceDirect

Redox Biology

journal homepage: www.elsevier.com/locate/redox

Deficient immunoproteasome assembly drives gain of α-synuclein pathology in Parkinson's disease

Mingxia Bi [a], Xixun Du [a], Xue Xiao [a], Yingying Dai [a], Qian Jiao [a], Xi Chen [a], Lingqiang Zhang [b], Hong Jiang [a,*]

[a] Department of Physiology, Shandong Provincial Key Laboratory of Pathogenesis and Prevention of Neurological Disorders and State Key Disciplines: Physiology, School of Basic Medicine, Medical College, Qingdao University, Qingdao, China
[b] State Key Laboratory of Proteomics, National Center for Protein Sciences (Beijing), Beijing Institute of Lifeomics, Beijing, China

ARTICLE INFO

Keywords:
Parkinson's disease
α-synuclein
Immunoproteasome
POMP
NRF2

ABSTRACT

Aberrant α-synuclein (α-Syn) accumulation resulting from proteasome dysfunction is considered as a prominent factor to initiate and aggravate the neurodegeneration in Parkinson's disease (PD). Although the involvement of 26S proteasome in proteostasis imbalance has been widely accepted, our knowledge about the regulation of immunoproteasome function and its potential role in α-Syn pathology remains limited. Immunoproteasome abundance and proteolytic activities depend on the finely tuned assembly process, especially β-ring formation mediated by the only well-known chaperone proteasome maturation protein (POMP). Here, we identified that α-Syn overexpression was associated with a reduction in immunoproteasome function, which in turn limited the degradation of polo-like kinase 2 (PLK2), exacerbated α-Syn Ser129 phosphorylation and aggregation, ultimately leading to the neurodegeneration. These effects could be dramatically attenuated by β5i overexpression. Mechanistically, α-Syn suppressed the transcriptional regulation of POMP by nuclear factor erythroid 2-related factor 2 (NRF2), thereby preventing the assembly of immunoproteasome β subunits. Dopaminergic neurons-specific overexpression of NRF2-POMP axis effectively rescued the aggregation of α-Syn and PD-like phenotypes. These findings characterized abnormal immunoproteasome assembly as a key contributor governing α-Syn accumulation and neurodegeneration, which might open up a new perspective for the implication of immunoproteasome in PD and provide approaches of manipulating immunoproteasome assembly for therapeutic purposes.

1. Introduction

Parkinson's disease (PD) is an age-related neurodegenerative disorder. The gradual, irreversible loss of substantia nigra (SN) dopaminergic neurons and the resulting striatal dopamine depletion account for the motor symptoms of PD [1,2]. Pathologically, intracellular protein aggregates primarily composed of α-synuclein (α-Syn) in Lewy bodies serve as the neuropathological hallmark of PD [3,4]. α-Syn, a natively unfolded, small peripheral protein (140 amino acids), can transition between different conformations, including native monomers, potentially toxic oligomers and fibrils. More importantly, a dramatic phosphorylated α-Syn at Ser129 (>90%) has been observed within Lewy bodies, suggesting that this post-translational modification may account for α-Syn aggregation and Lewy bodies formation [5,6]. Polo-like kinase 2 (PLK2), the main kinase responsible for α-Syn Ser129 phosphorylation, is significantly increased in the brain and serum of PD patients [7,8]. However, whether Ser129 phosphorylation promotes or suppresses α-Syn accumulation and neurotoxicity remains in debate. In this regard, what drives the aberrant aggregation of α-Syn will continue to be intensive topics of PD pathogenesis research.

It is generally accepted that the disruption of proteasomal degradation is linked to aberrant protein accumulation, which probably overload the cellular elimination capacity rendering dopaminergic neurons susceptible to injury [9]. Proteasome, in collaboration with a refined ubiquitin system, selectively degrades short-lived proteins as well as misfolded or damaged proteins. There mainly exists 26S proteasome and immunoproteasome in the central nervous system. Upon certain stimulus, three catalytic subunits β1, β2, and β5 can be replaced by their homologues β1i, β2i, and β5i to form immunoproteasome [10]. Up to now, the defects in the structure, function and regulation of 26S

* Corresponding author.
E-mail address: hongjiang@qdu.edu.cn (H. Jiang).

https://doi.org/10.1016/j.redox.2021.102167
Received 5 September 2021; Received in revised form 11 October 2021; Accepted 13 October 2021
Available online 14 October 2021

proteasome in PD patients have been widely reported [11,12]. However, the functional role of immunoproteasome and its potential effects on dopaminergic neurons remain in part unknown. Immunoproteasome should no longer be thought of only generating peptides for antigen presentation, so does its important role in antioxidant stress and proteostasis maintenance by eliminating oxidatively damaged proteins [13,14]. Enhanced proteolytic activities of immunoproteasome is required for efficient degradation of poly-ubiquitylated proteins upon oxidative stress [15]. It is probable that immunoproteasome deficiency is involved in PD pathogenesis characterized by abnormal protein aggregation.

Immunoproteasome function depends on a complex and tightly regulated assembly process, in which all subunits must be properly combined to form an active complex [16]. The incorporation of catalytic subunits β1i, β2i, and β5i into 20S core particle leads to the enhanced proteolytic activities and improved accessibility for protein substrates. The only well-described chaperone dedicated to β-ring assembly is proteasome maturation protein (POMP) [17]. The mechanisms for assembling different types of proteasome are roughly similar, except that POMP has a greater affinity for β5i than β5 subunit [18]. Interferon-γ (IFN-γ) stimulates the biosynthesis of POMP, resulting in the assembly of immunoproteasome occurs preferentially and more quickly than 26S proteasome [19]. Besides, loss of POMP leads to the incoordination of β-ring assembly, which in turn impairs immunoproteasome function. Previous studies have shown that POMP is transcriptionally regulated by nuclear factor erythroid 2-like 2 (NRF2) and NRF3, consequently enhancing the peptide-hydrolyzing activities and protein degradation [20]. Considering that coordinated catalytic subunits expression is critical for immunoproteasome abundance and activity, it is necessary to understand the molecular mechanisms regulating β-ring assembly and the implications of immunoproteasome in PD.

In this study, we investigate the involvement of immunoproteasome dysfunction in PD pathogenesis and further explore its underlying mechanisms. We first screened for the alterations in immunoproteasome function upon exposure to α-Syn and the potential effects on dopaminergic neurons by targeting PLK2 degradation. Then, we explored whether α-Syn-induced immunoproteasome dysfunction was attributed to the deficiency of POMP-mediated β-ring assembly. The present study expands our current knowledge about the implication of immunoproteasome in PD models and provides evidence for enhancing immunoproteasome assembly as a novel therapeutic approach.

2. Materials and methods

2.1. Plasmids and viruses

The Flag tagged WT α-Syn and A53T α-Syn were constructed by cloning the cDNA of the full-length or mutant derivatives into the XhoI/KpnI sites of the pCMV-Tag2A-Flag vector. The plasmids HA-β5i, His-Ub, Myc-PLK2, and Myc-NRF2 were purchased from OBiO Technology (Shanghai, China). The siRNA-β5i, sh-NRF2, and sh-POMP were purchased from Genechem Technology (Shanghai, China).

2.2. Cell culture and transfection

SH-SY5Y cells were purchased from National Infrastructure of Cell Line Resource (Shanghai, China) and cultured in MEM/F12 medium supplemented with 15% fetal bovine serum (Gibco, Grand Island, NY, USA) and 1% penicillin-streptomycin at 37 °C with 5% CO_2. Cell transfection was performed by Lipofectamine 2000 (Invitrogen, Waltham, MA, USA) reagent according to the manufacturer's protocol.

2.3. Animals

Mutant human A53T α-Syn transgenic mice (B6; C3-Tg(Prnp-*SNCA**A53T) 83Vle/J) were purchased from the Jackson Laboratory. Animals were maintained in controlled temperature and humidity rooms on a 12 h light/dark cycle with free access to food and water. Male homozygous A53T α-Syn transgenic mice and their wild type littermates were used for the following experiments. Animal experiments were carried out according to the guidelines of National Institutes of Health Guidelines for the Care and Use of Laboratory Animals. All protocols were approved by the Animal Ethics Committee of Qingdao University.

2.4. Stereotaxic injection of adeno-associated virus (AAV)

AAV-Slc6a3-β5i, AAV-Slc6a3-NRF2 or AAV-Slc6a3-POMP purchased from Hanbio Technology (Shanghai, China) was injected into the SN (1 μL per hemisphere at 0.2 μL/min) with the following coordinates: anteroposterior (AP) = −3.2 mm, mediolateral (ML) = ±1.3 mm, dorsoventral (DV) = −4.6 mm from bregma. At the end of injection, the needle was retained for another 5 min for a complete absorption of the solution. After surgery, animals were monitored and post-surgical care was provided. For biochemical experiments, the SN was immediately isolated and frozen at −80 °C. For histological experiments, mice were perfused with 4% paraformaldehyde (PFA) and brains were sliced for immunofluorescence staining.

2.5. RNA-Seq procedures and bioinformatic analysis

RNA-Seq library preparation and ultra-sequencing were performed by Novogene (Beijing, China) according to Illumina's protocols. Total RNA samples from WT α-Syn and A53T α-Syn transfected SH-SY5Y cells were isolated using TRIzol reagent (Invitrogen, Waltham, MA, USA). Constructed libraries were validated and quantified using automated electrophoresis system (BioRad) and PCR, respectively. Differentially expressed genes (DEGs) were determined using the edgeR package and the significance was defined according to the combination of log2-fold change ≥ 1 and P value ≤ 0.05. Heatmap visualization and DEGs cluster were done after counting the gene expression values in standard deviation and using hierarchical clustering with average linkage. GO and pathway enrichment analysis were based on the Gene Ontology Database (http://www.geneontology.org/) and KEGG pathway database (http://www.genome.jp/kegg/), respectively.

2.6. Real-time PCR

Total RNA was isolated using the TRIzol Reagent (Invitrogen, Waltham, MA, USA) according to the manufacturer's instructions. 1 μg RNA was used for cDNA synthesis in a 20 μL reaction with the reverse-transcription kit (Takara Biomedical Technology, Beijing, China). Quantitative real-time PCR was carried out using SYBRGreen Master Mix (Takara Biomedical Technology, Beijing, China). The expression of each gene was normalized to GAPDH. The primer sequences were displayed in Table S3.

2.7. Co-IP and Western blot

Cells were washed with ice cold 0.01 M PBS and lysed in HEPES buffer (20 mM HEPES, pH 7.2, 50 mM NaCl, 1 mM NaF, 0.5% Triton X-100) supplemented with protease inhibitor cocktail (Roche). The lysates were sonicated (amplitude 15%, push-on time 5 s, and push-off time 2 s), and then centrifugated at 12,000 rpm for 10 min at 4 °C to collect the supernatant. For immunoprecipitation, the protein A/G plus-agarose beads (Santa Cruz Biotechnology, Dallas, TX, USA) were added to the samples for preclearing at 4 °C for 2 h. After centrifugation at 3000 rpm for 5 min at 4 °C, the supernatant was incubated with the indicated antibodies followed by incubation for 4–6 h at 4 °C. The protein A/G plus-agarose beads were added and incubated for another 8–10 h. After extensive washing, the beads resolved with sodium dodecyl sulfate-polyacrylamide gel electrophoresis (SDS-PAGE) loading buffer were boiled for 5 min. The samples were then subjected to immunoblotting

with the indicated antibodies. Primary and secondary antibodies used in this study were listed in Table S4.

2.8. In vitro ubiquitin conjugation assay

Fifty-microgram SH-SY5Y cell lysates were incubated with 1 mM HA-tagged Ub for 1 h in reaction buffer containing 20 mM Tris-HCl (pH 7.5), 20 mM KCl, 5 mM $MgCl_2$, 10% glycerol, 1 mM DTT, 50 mM MG-132, and 5 mM ub-aldehyde (Boston Biochemicals, Ashland, USA). Ub conjugates were immunoblotted by HA antibody.

2.9. Measurement of immunoproteasome proteolytic activities

The immunoproteasome chymotrypsin-like and trypsin-like activities were assessed using fluorogenic peptide substrates Suc-LLVY-AMC and Z-ARR-AMC, respectively. Briefly, protein concentration was adjusted to 1 μg/μL, and 3 μL lysate was added to 97 μL reaction buffer (50 mM HEPES, 5 mM EDTA, 150 mM NaCl and 1% TX-100) and 50 μM fluorogenic substrates for 1 h at 37 °C. To confirm the specificity of immunoproteasome activities, we analyzed proteolytic activities in the presence or absence of selective β1i inhibitor ML604440 (MCE, 500 nM) and β5i inhibitor ONX0914 (MCE, 500 nM), respectively. The inhibitor was premixed with cell lysate for 10 min before the reaction was started. Finally, the reaction was monitored with excitation at 380 nm and emission at 460 nm using a microplate reader (Molecular Device, M5, San Jose, CA, USA). The hydrolysis of fluorogenic substrates in the inhibitor-treated samples was subtracted from that of the inhibitor-untreated samples to represent immunoproteasome proteolytic activities.

2.10. TritonX-100 (TX-100) soluble and insoluble α-syn analysis

Tissues dissected from A53T α-Syn transgenic mice were resuspended in ice-cold TX-100 lysis buffer (50 mmol/L Tris pH 7.4, 175 mmol/L NaCl, 5 mmol/L EDTA, 1% TX-100, 1 mmol/L PMSF), and incubated on ice for 30 min. After centrifuging at 100,000 g for 30 min at 4 °C, the resulting supernatant was TX-100 soluble fraction. The pellets were resuspended in lysis buffer containing 2% SDS. After sonication on ice, the collection was designated as the TX-100 insoluble fraction.

2.11. Thioflavin T (ThT) fluorescence assay

Aliquots of 5 μL tissue lysates were diluted to 100 mL with 25 mM ThT in PBS, and then incubate for 10 min at room temperature. At the end of treatment, the fluorescence was assessed at 450 nm excitation and 510 nm emission using a microplate reader (Molecular Device, M5, San Jose, CA, USA).

2.12. Immunofluorescence staining

SH-SY5Y cells were seeded on fibronectin-coated glass coverslips in 24-well plates and brains were sliced into 20 mm-thick sections. After fixation in 4% PFA overnight followed by blocking with 10% goat serum, mouse anti-tyrosine hydroxylase (TH) (1:500) and rabbit anti-pS129 α-Syn (1:200) were incubated overnight at 4 °C. The cells or tissues were then washed with PBS and incubated with the secondary antibodies Alexa Fluor® 555 goat anti-mouse IgG (H + L) (1:500), Alexa Fluor® 488 goat anti-rabbit IgG (H + L) (1:500) and Alexa Fluor® 555 goat anti-rabbit IgG (H + L) (1:500) for 1 h at room temperature and then added DAPI for 5 min before mounted with antifade solution. Images were acquired using immunofluorescent microscopy (Observer A1, Zeiss, Germany). The number of TH-positive neurons in the SN was determined using stereological quantification as previously described [21].

2.13. Luciferase reporter assay

Human POMP promoter sequence was cloned in pGL-3 vector. Cells were cultured in 96-well plates and transfected with the POMP promoter construct along with the pRLCMV Renilla luciferase reporter plasmid as an internal control. At the end of treatment, cells were collected with 500 μL 1 × PLB buffer and gently shake for 20 min. Then, the PLB lysates were dispensed into 96-well plate (20 μL per well). Add the luciferase assay substrate and measure the Firefly and Renilla luciferase activities using the dual-luciferase reporter system (Promega Corporation, Madison, USA) The relative luciferase activity was normalized using Renilla luciferase.

2.14. Cell viability assessment

Cell viability was measured using 3-(4,5-dimethyl-2-thiazolyl)-2,5-diphenyl-2-H-tetrazolium bromide (MTT) assay. SH-SY5Y cells were seeded in 96-well plates and at the end of treatment, the culture medium was replaced with the medium containing MTT at a final concentration of 5 mg/mL for 4 h at 37 °C. Then, the insoluble formazan was dissolved with dimethyl sulfoxide (DMSO). Measure the absorbance at 494 nm and 630 nm using a microplate reader (Molecular Device, M5, San Jose, CA, USA).

2.15. Flow cytometric measurement of mitochondrial membrane potential and ROS

Changes in mitochondrial membrane potential and ROS generation in α-Syn overexpressing SH-SY5Y cells were measured using flow cytometry as previously described [22]. In brief, cells were washed with HBS three times followed by incubation with 5 mM Rhodamine123 (Rh123) or 5 mM 2′,7′-dichlorofluorescein diacetate (H_2DCFDA) for 30 min at 37 °C in dark. For analysis, 488 nm excitation and 525 nm emission wavelengths were used to assess 10,000 cells and the fluorescence intensity was analyzed using CellQuest Software.

2.16. Rotarod test and pole test

A rotarod apparatus (Med Associates, USA) was used to measure the balance and motor coordination. During the training period, mice were allowed to adapt the rotarod for 2 min without rotation. Then, the drum was slowly accelerated to a speed of 4–40 rpm for a maximum of 5 min. The latency to fall off the rotarod within this time period was recorded. In pole test, mice were placed facing upwards at the top of a pole wrapped with bandage gauze (60 cm long and 1 cm diameter). The mice were trained to turn to orient downward and traverse the pole into the bottom. Then, the time used to turn to orient downward and the total time to reach the base of the pole were recorded.

2.17. Statistical analysis

One-way analysis of variance (ANOVA) followed by the Student-Newman-Keuls test was used for comparing the difference in more than two groups. Data are presented as mean ± SEM and analyzed by GraphPad Prism 8.0 (GraphPad Software Inc.). A probability of $P < 0.05$ was considered statistically significant.

3. Results

3.1. Immunoproteasome function was impaired in PD models

RNA-Seq was performed to analyze the proteasome subunits expression profiles in WT α-Syn and A53T α-Syn overexpressed SH-SY5Y cells (Fig. 1A and Table S1). Total 483 DEGs were identified including 80 upregulated and 403 downregulated genes in A53T α-Syn group compared with control (Fig. S1A) and 398 DEGs including 72

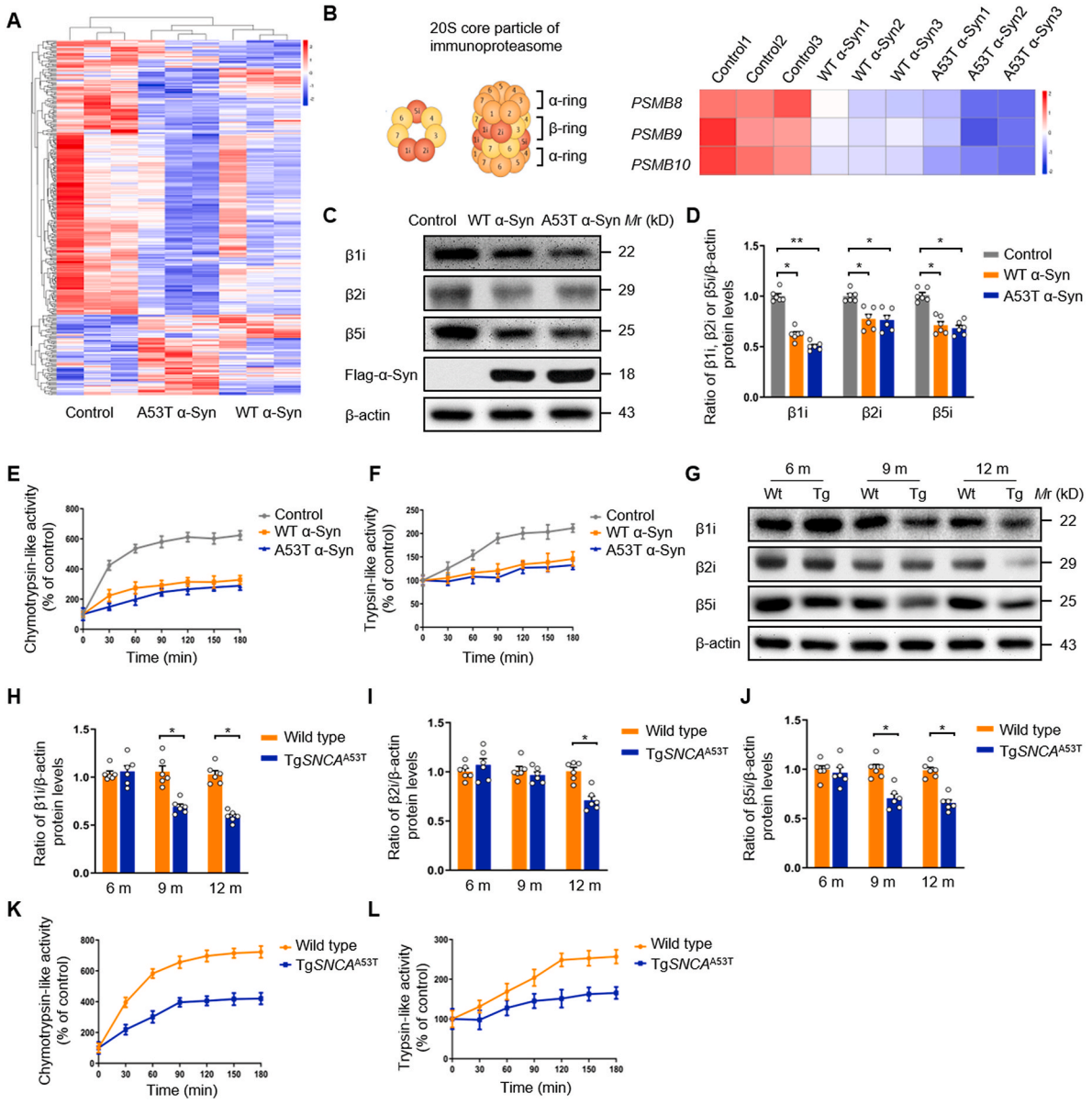

Fig. 1. Immunoproteasome function is inhibited in α-Syn overexpressed SH-SY5Y cells and A53T α-Syn transgenic mice. **(A)** Cluster of gene expression profiles in WT α-Syn or A53T α-Syn overexpressed SH-SY5Y cells graphed as heatmap. **(B)** The constitution of 20S core particle of immunoproteasome and DEGs associated with immunoproteasome β1i *(PSMB9)*, β2i *(PSMB10)*, and β5i *(PSMB8)* were visualized using heatmap. The protein levels of immunoproteasome β1i, β2i and β5i subunits were determined by Western blot in SH-SY5Y cells **(C, D)** and in the SN of A53T α-Syn transgenic mice **(G–J)**. Chymotrypsin-like **(E, K)** and trypsin-like **(F, L)** activity were measured by fluorescence from the breakdown of Suc-LLVY-AMC and Z-ARR-AMC fluorogenic substrate, respectively. $^{*}P < 0.05$, $^{**}P < 0.01$.

upregulated and 326 downregulated genes were obtained in WT α-Syn group compared with control (Fig. S1B). Only 166 DEGs were found in A53T α-Syn group compared with WT α-Syn group, indicating little difference between these two groups (Fig. S1C). Further analysis with KEGG pathway indicated that these DEGs were significantly enriched in proteasome, ubiquitin-mediated proteolysis, antigen processing and presentation et al. (Figs. S1D–F). Of note, the abundance of β1i (*PSMB9*), β2i (*PSMB10*), and β5i (*PSMB8*), three catalytic subunits of immunoproteasome, were found to be down-regulated in the presence of α-Syn (Fig. 1B and Table S2).

We further validated the expression of DEGs both in vitro and in vivo. In WT α-Syn or A53T α-Syn transfected SH-SY5Y cells, β1i, β2i, and β5i expression were significantly decreased (Fig. 1C and 1D). β1i and β5i catalytic subunits exert chymotrypsin-like proteolytic activity, while β2i shows trypsin-like activity. As expected, both the chymotrypsin-like (Fig. 1E) and trypsin-like activity (Fig. 1F) were declined in α-Syn overexpressed SH-SY5Y cells. Similar results were obtained in A53T α-Syn transgenic mice, which express human full-length A53T variant α-Syn and exhibit the widely distributed α-Syn inclusions accompanied by the progressive motor phenotypes at the age of 6–12 months. In the present study, we observed that the expression of β1i (Fig. 1G and 1H) and β5i (Fig. 1G and 1J) in the SN was decreased in 9 and 12-month A53T α-Syn transgenic mice and the nigral β2i was reduced in 12-month A53T α-Syn transgenic mice (Fig. 1G and 1I). Moreover, the chymotrypsin-like (Fig. 1K) and trypsin-like activity (Fig. 1L) in the SN of 12-month A53T α-Syn transgenic mice were much lower than those in their wild-type littermates. These results uncover a significant decrease in immunoproteasome function including impaired catalytic subunits expression and proteolytic activities in PD models.

3.2. Immunoproteasome promotes the degradation of PLK2

Besides the role of immunoproteasome in antigen presentation, it also possesses the ability to degrade poly-ubiquitylated proteins which do not differ with 26S proteasome [23]. PLK2, as the main kinase for α-Syn Ser129 phosphorylation, undergoes ubiquitylation by E3 ubiquitin ligase ring finger protein 180 (RNF180) to control glioma development [24]. To assess whether immunoproteasome participated in the degradation of PLK2, we first examined the interactions between β5i and PLK2. As depicted in Fig. 2A, endogenous PLK2 was immunoprecipitated by antibody against β5i in SH-SY5Y cells, but not by the non-specific IgG control. Similarly, endogenous β5i was immunoprecipitated by PLK2 antibody in SH-SY5Y cells (Fig. 2B). Next, SH-SY5Y cells were transfected with Myc-tagged PLK2 and HA-tagged β5i. Co-IP assay showed that Myc-PLK2 was readily detected in the fractions of immunoprecipitation with anti-HA antibody (Fig. 2C) and HA-β5i was immunoblotted in anti-Myc immunoprecipitates (Fig. 2D), suggesting that β5i directly interacted with PLK2.

Considering that β5i overexpression or depletion had no significant effects on PLK2 mRNA levels (Fig. 2E and F), we asked whether β5i regulated the ubiquitin-proteasome degradation of PLK2. Ubiquitylation assay showed that β5i overexpression significantly enhanced the ubiquitylation level of PLK2 (Fig. 2G), whereas β5i knockdown had the opposite effects (Fig. 2H). Additionally, the protein levels of PLK2 were found to be decreased in SH-SY5Y cells overexpressing β5i (Fig. 2I and J), however, PLK2 protein expression was increased in SH-SY5Y cells with β5i knockdown (Fig. 2K and L). Next, we performed PLK2 half-life analysis in SH-SY5Y cells treated with 10 μg/mL protein synthesis inhibitor cycloheximide (CHX). The half-life of PLK2 was shortened in cells overexpressing β5i (Fig. 2M and N), but prolonged in cells depleted of β5i (Fig. 2O and P), indicating that β5i negatively regulated the protein stability of PLK2. Collectively, these observations indicate that PLK2 was a previously unrecognized substrate for immunoproteasome, which was responsible for the maintenance of PLK2 protein stability.

3.3. Immunoproteasome dysfunction exacerbates α-Syn phosphorylation and aggregation

The increased immunoreactivity of phosphorylated α-Syn at Ser129 was detectable both in SH-SY5Y cells (Fig. 3A) and in the SN of 9 and 12-month A53T α-Syn transgenic mice (Fig. S2A and S2B). We also observed the aggregation of α-Syn in the SN of 9 and 12-month A53T α-Syn mice as indicated by ThT fluorescence (Fig. S2C). These pathological features were coincided with the severe damage both in vivo and in vitro, including an increase in ROS generation (Fig. S2E), a decrease in mitochondrial transmembrane potential (Fig. S2F) and cell viability (Fig. S2G), reduced TH protein levels (Fig. S2H and S2I) and impaired motor coordination (Fig. S2J-S2L). Then, we asked whether α-Syn-induced neurodegeneration arose from impaired immunoproteasome function. α-Syn overexpression in SH-SY5Y cells caused a significant decrease in β5i expression and a corresponding increase in the protein levels of PLK2 (Fig. 3B and C). In 12-month A53T α-Syn transgenic mice, the nigral PLK2 expression was also found to be increased (Fig. 3E and F). Since PLK2 is reported as a kinase to phosphorylate α-Syn, we further observed an increase in α-Syn Ser129 phosphorylation in SH-SY5Y cells (Fig. 3B and D) and A53T α-Syn transgenic mice (Fig. 3E and G). Under the condition of β5i overexpression, elevated PLK2 protein levels and α-Syn Ser129 phosphorylation were partially reversed both in SH-SY5Y cells (Fig. 3B and D) and 12-month A53T α-Syn transgenic mice (Fig. 3E-H). Notably, when SH-SY5Y cells were pre-incubated with PLK2 small-molecule inhibitor BI2536 (Selleck, 1 μmol/L) for 30 min, and then co-treated with HA-β5i for 24 h, we observed that α-Syn Ser129 phosphorylation was further mitigated when compared with β5i overexpression groups (Fig. 3B and D). These data indicate that immunoproteasome dysfunction aggravates α-Syn Ser129 phosphorylation via preventing PLK2 degradation.

Next, we wondered PLK2-induced α-Syn Ser129 phosphorylation enhanced or suppressed α-Syn aggregation and neurotoxicity. In α-Syn transfected SH-SY5Y cells, an accumulation of α-Syn in TX-100 insoluble fraction was detectable (Fig. 3I and J). Moreover, BI2536 treatment further reduced TX-100 insoluble α-Syn levels when compared with β5i overexpression groups, suggesting that PLK2-mediated α-Syn Ser129 phosphorylation further promotes the aggregation of α-Syn. Similarly, TX-100 insoluble form of α-Syn in the SN of 12-month A53T α-Syn transgenic mice was increased (Fig. 3K and L). We also observed the aggregation of α-Syn in the SN of 12-month A53T α-Syn mice as indicated by ThT fluorescence (Fig. 3M). Moreover, loss of nigral dopaminergic neurons (Fig. 3N and O) and decreased nigral TH protein levels were found in A53T α-Syn transgenic mice (Fig. 3P and Q). After the microinjection of dopaminergic neurons-specific virus containing the genes for β5i, nigral TX-100 insoluble α-Syn levels and dopaminergic neurons deletion could be dramatically restored. The above results illuminate that immunoproteasome dysfunction suppresses PLK2 degradation, which further aggravates α-Syn Ser129 phosphorylation and aggregation in PD models.

3.4. α-Syn perturbs POMP-mediated immunoproteasome β-ring assembly

We next investigated the mechanism by which α-Syn negatively regulated immunoproteasome function. POMP is the only known chaperone that facilitates the assembly and maturation of β-ring. In the present study, we observed that both the mRNA and protein levels of POMP were found to be decreased in WT α-Syn or A53T α-Syn overexpressed SH-SY5Y cells (Fig. 4A-C). Consistently, the down-regulation of POMP was observed in the SN of 9 and 12-month A53T α-Syn transgenic mice (Fig. 4D-F). According to the Co-IP experiments, a stronger interaction between POMP and β-subunits was detected, and it was the precursor forms of β1i and β5i that could bind with POMP in SH-SY5Y cells (Fig. 4G). Torin1, as a positive control, has been reported to drastically suppress the maturation of immunoproteasome β5i subunit [25]. As shown in Fig. 4H, the binding of POMP to β5i precursor was significantly decreased under the condition of α-Syn overexpression. Subsequently, the mature forms of β1i and β5i were found to be reduced in α-Syn-transfected SH-SY5Y cells, which could be further aggravated by POMP knockdown (Fig. 4I-K). In the presence of α-Syn, improper assembly of immunoproteasome β-ring could cause defects in the chymotrypsin-like (Fig. 4L) and trypsin-like activity (Fig. 4M). This phenomenon could be further exacerbated by the deletion of POMP. Based on these findings, we conclude that α-Syn suppresses the expression of POMP, and then the decreased binding of POMP to β5i precursor inhibits immunoproteasome β-ring maturation, further highlighting the importance of POMP-mediated assembly for immunoproteasome function.

3.5. Enhancement of NRF2-POMP axis ameliorates α-Syn neurotoxicity

The expression of POMP is transcriptionally regulated by NRF2 and NRF3 by binding to specific sequences of POMP promoter, thereby facilitating the assembly of proteasome [26,27]. NRF2 and NRF3 belong to the transcription factors CNC family along with NRF1. Based on the RNA-Seq results, we found that only NRF2 mRNA and protein levels were decreased, whereas there was no obvious change in NRF1 and NRF3 expression (Fig. S3A-S3H), implying that NRF2 might account for the down-regulation of POMP by α-Syn. In NRF2-overexpressed HEK293T cells, the construct containing POMP promoter region, but not lacking NRF2 binding sites and ARE sequence, exhibited the highest luciferase intensity (Fig. 5A and B). Furthermore, overexpression of NRF2 induced the expression of POMP at both mRNA and protein levels (Fig. S3I-S3K). NRF2 knockdown exhibited a significant decrease in relative luciferase activity (Fig. 5C) and POMP expression (Fig. S3L-S3N), indicating that NRF2 transcriptionally regulated POMP.

In the presence of α-Syn, the transcriptional activity of NRF2 was

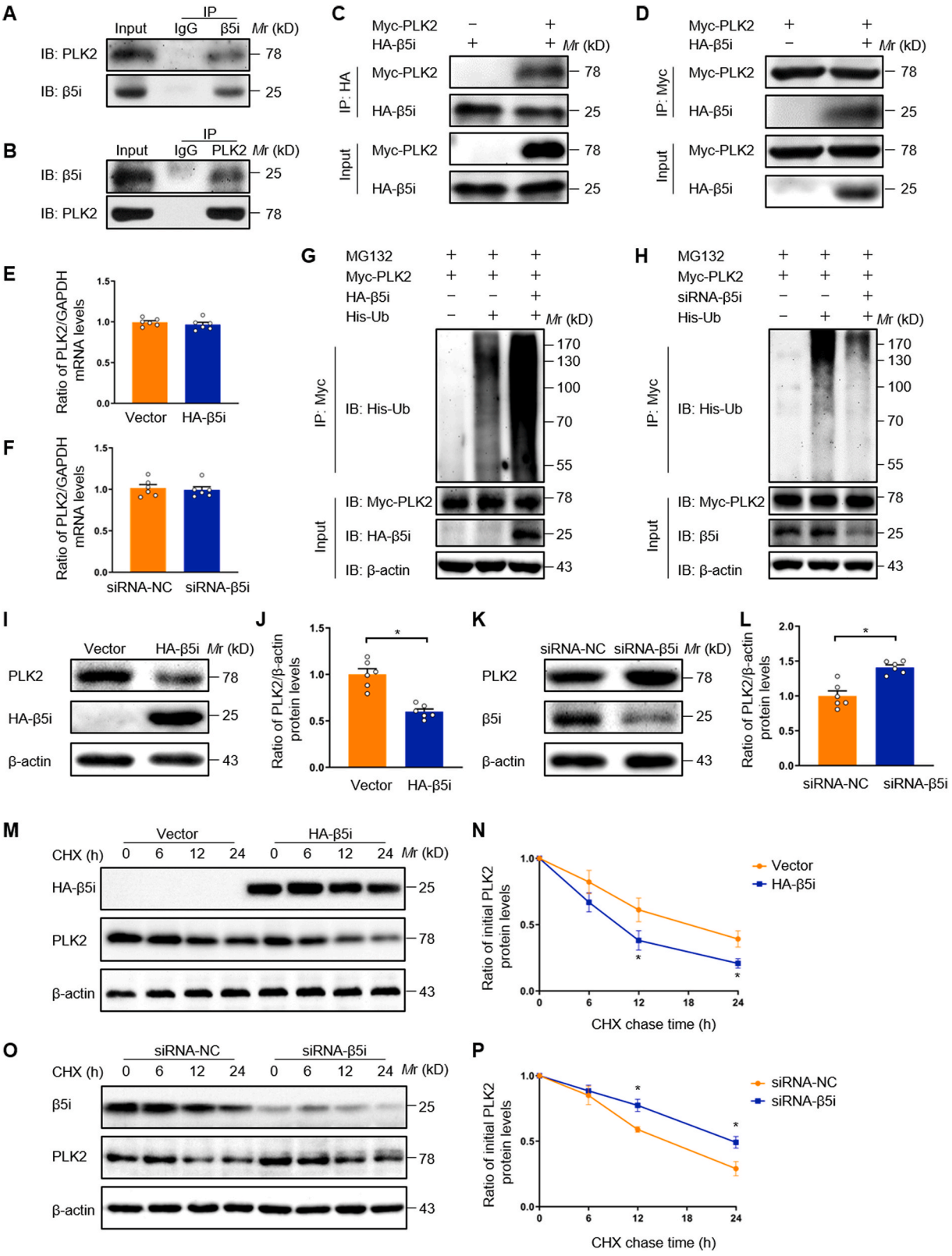

Fig. 2. β5i interacts with PLK2 and participates in its degradation. **(A, B)** Endogenous interactions between β5i and PLK2 were determined in SH-SY5Y cells immunoprecipitated with anti-β5i or anti-PLK2 antibody and analyzed by Western blot to detect PLK2 and β5i protein levels. **(C, D)** SH-SY5Y cells were transfected with the indicated plasmids. The interactions between β5i and PLK2 were determined by immunoprecipitation with anti-HA or anti-Myc antibody and analyzed by Western blot with the indicated antibodies. **(E, F)** The mRNA levels of PLK2 in SH-SY5Y cells with β5i overexpression or β5i knockdown were determined by real-time PCR. **(G, H)** The ubiquitylation levels of PLK2 in SH-SY5Y cells with β5i overexpression or β5i knockdown were examined by in vitro ubiquitin conjugation assay. The protein levels of PLK2 in SH-SY5Y cells with β5i overexpression **(I, J)** or β5i knockdown **(K, L)** were determined by Western blot. The half-life of PLK2 was assesses in SH-SY5Y cells with β5i overexpression **(M, N)** or β5i knockdown **(O, P)** treated with 10 μg/mL CHX for the indicated time. $^*P < 0.05$.

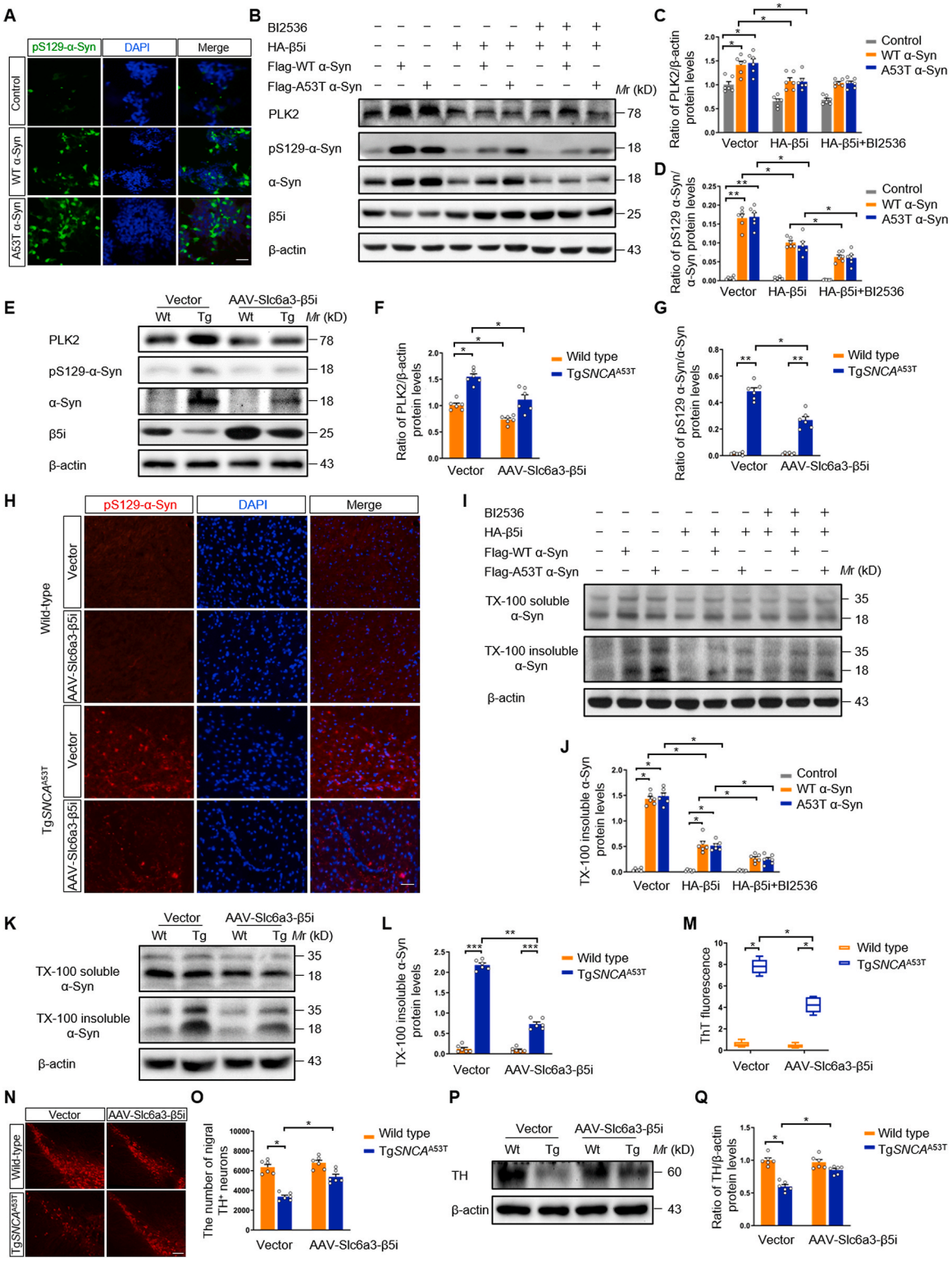

Fig. 3. Immunoproteasome deficiency induces α-Syn phosphorylation and accumulation. **(A)** Immunostaining of pS129 α-Syn in WT α-Syn or A53T α-Syn transfected SH-SY5Y cells. The protein levels of PLK2, pS129 α-Syn in β5i overexpressed SH-SY5Y cells in the presence or absence of BI 2536 **(B–D)** and in the SN of 12-month A53T α-Syn transgenic mice with dopaminergic neurons-specific β5i overexpression **(E–G)**. **(H)** Immunofluorescence was applied to observe nigral pS129 α-Syn in 12-month A53T α-Syn transgenic mice with dopaminergic neurons-specific β5i overexpression. The soluble and insoluble α-Syn in β5i overexpressed SH-SY5Y cells in the presence or absence of BI 2536 **(I, J)** and in the SN of 12-month A53T α-Syn transgenic mice with dopaminergic neurons-specific β5i overexpression **(K, L)**. **(M)** The aggregation of α-Syn was detected by ThT immunofluorescence in the SN of 12-month A53T α-Syn transgenic mice with dopaminergic neurons-specific β5i overexpression. Representative immunofluorescent images of TH staining **(N)** and stereological quantification of TH-positive neurons **(O)** in the SN of 12-month A53T α-Syn transgenic mice with dopaminergic neurons-specific β5i overexpression. **(P, Q)** western blot was conducted to detect nigral TH protein levels in 12-month A53T α-Syn transgenic mice with dopaminergic neurons-specific β5i overexpression. Scale bar = 100 μm $^{*}P < 0.05$, $^{**}P < 0.01$, $^{***}P < 0.001$.

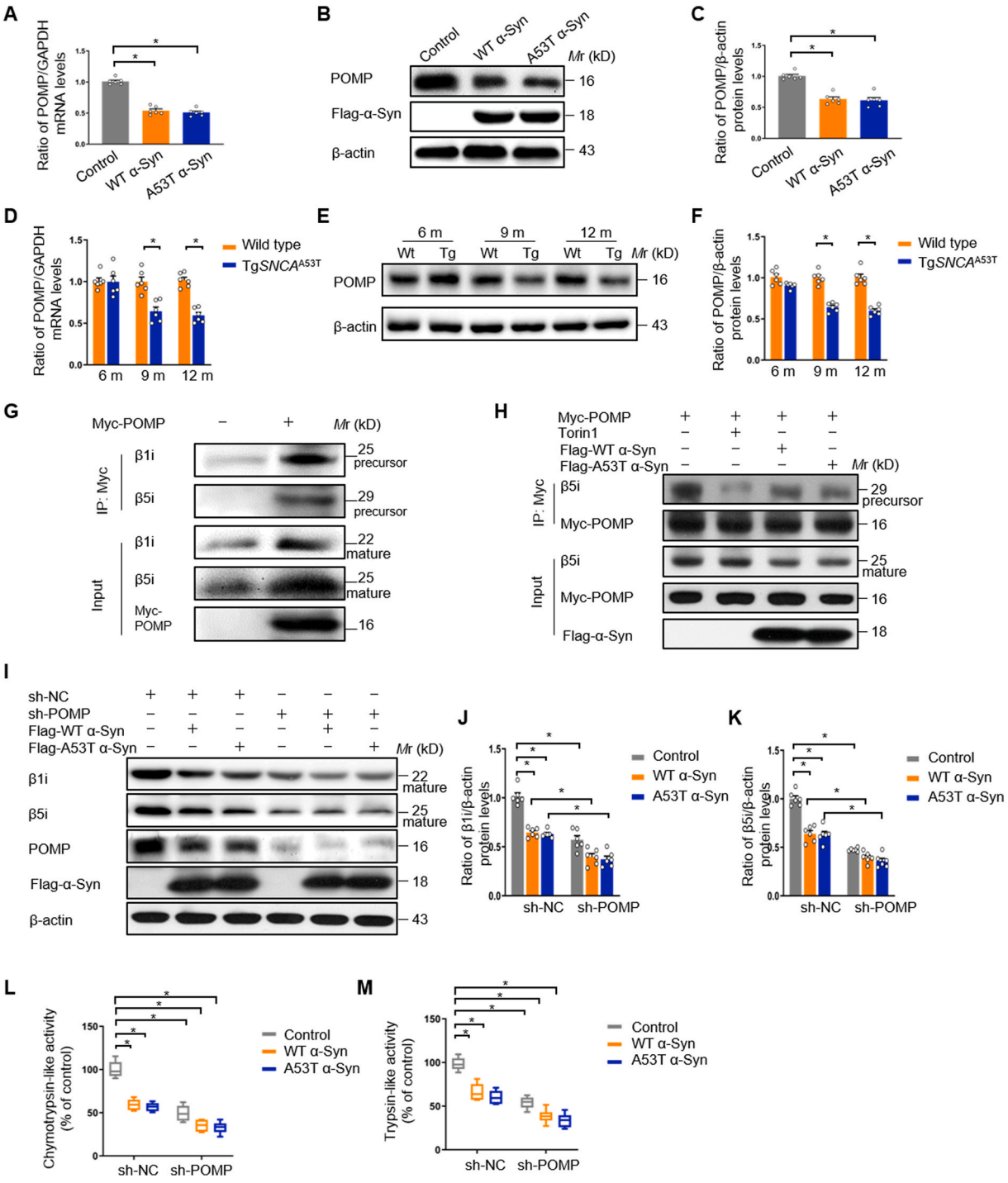

Fig. 4. Loss of POMP induced by α-Syn disturbs immunoproteasome β-ring assembly. POMP mRNA and protein levels in WT α-Syn or A53T α-Syn transfected SH-SY5Y cells **(A–C)** and in the SN of 12-month A53T α-Syn transgenic mice **(D–F)**. **(G)** The interaction between β1i, β5i precursors and POMP in SH-SY5Y cells was examined immunoprecipitated with anti-Myc antibody. The whole-cell lysate was subjected to immunoblot with anti-β1i, anti-β5i and anti-Myc antibody. **(H)** The interaction between β5i precursor and POMP was detected in WT α-Syn or A53T α-Syn transfected SH-SY5Y cells immunoprecipitated with anti-Myc antibody. The whole-cell lysate was subjected to immunoblot with anti-β5i, anti-Myc and anti-Flag antibody. **(I–K)** The protein levels of β1i and β5i were determined by Western blot in WT α-Syn or A53T α-Syn transfected SH-SY5Y cells with POMP knockdown. **(L, M)** Chymotrypsin-like and trypsin-like activity were measured in WT α-Syn or A53T α-Syn transfected SH-SY5Y cells with POMP knockdown. $*P < 0.05$.

inhibited (Fig. S4A), resulting in the decrease in POMP and β1i, β5i subunits expression (Fig. S4B-S4E), accompanied by the lower proteolytic activities (Fig. S4F and S4G). Overexpression of NRF2 could dramatically rescue the loss of POMP expression and impaired immunoproteasome function. Consistently, in 12-month A53T α-Syn transgenic mice infected with dopaminergic neurons-specific AAV containing NRF2 or POMP, β1i and β5i expression were found to be up-regulated (Fig. 5D-F), accompanied by enhanced proteolysis activities (Fig. S3R and S3S) and the degradation of PLK2, leading to the decrease in PLK2 protein levels (Fig. 5D and G). Meanwhile, there was a decrease in α-Syn Ser129 phosphorylation (Fig. 5D and H), TX-100 insoluble α-Syn (Fig. 5I and J) and ThT fluorescence (Fig. 5K). Overexpression of NRF2-POMP

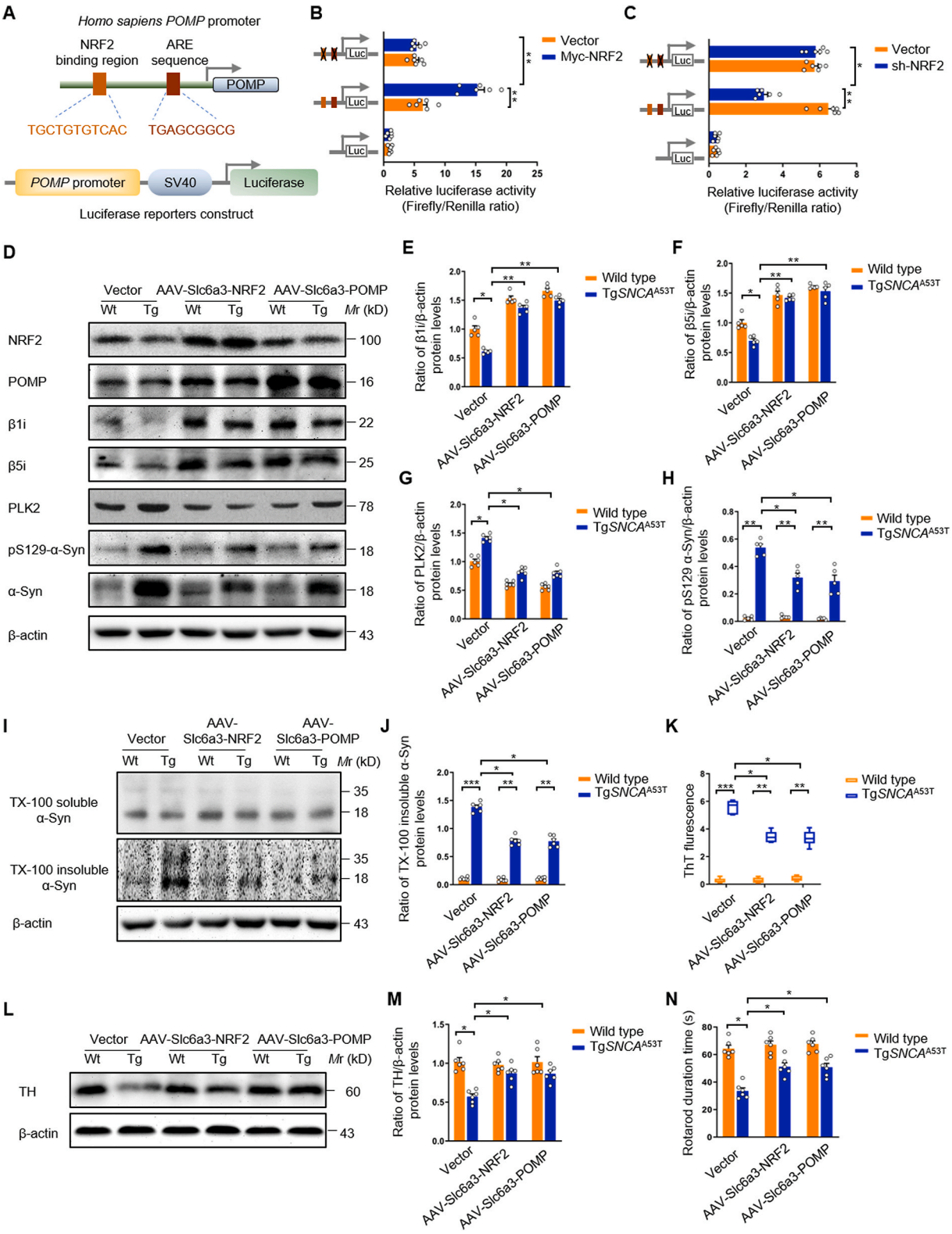

Fig. 5. Dopaminergic neurons-specific overexpression of NRF2-POMP axis alleviates α-Syn pathology. **(A)** *Homo sapiens POMP* promoter contains NRF2 binding region (TGCTGTGTCAC) and ARE sequence (TGAGCGGCG). **(B, C)** Dual-luciferase reporter assay was applied to detect the interaction between POMP promoter and NRF2. **(D–H)** Western blot was applied to detect the nigral protein levels of β1i, β5i, PLK2, pS129 α-Syn in 12-month A53T α-Syn transgenic mice with dopaminergic neurons overexpressing NRF2 or POMP. **(I, J)** The soluble and insoluble α-Syn levels were detected in the SN of 12-month A53T α-Syn transgenic mice with dopaminergic neurons overexpressing NRF2 or POMP. **(K)** α-Syn aggregation was detected by ThT immunofluorescence in the SN of 12-month A53T α-Syn transgenic mice with dopaminergic neurons overexpressing NRF2 or POMP. **(L, M)** Western blot was applied to detect the nigral TH in 12-month A53T α-Syn transgenic mice with dopaminergic neurons overexpressing NRF2 or POMP. **(N)** Rotarod test was used to evaluate the motor ability in 12-month A53T transgenic mice with dopaminergic neurons-specific overexpression of NRF2-POMP axis. $^{*}P < 0.05$, $^{**}P < 0.01$, $^{***}P < 0.001$.

axis antagonized the decreased TH protein levels in 12-month A53T α-Syn transgenic mice (Fig. 5L and M). Improved motor coordination was observed by rotarod test, where the time spent on the rotarod was increased upon dopaminergic neurons-specific overexpression of NRF2-POMP axis (Fig. 5N). As such, these data indicate that α-Syn-induced loss of POMP was due to the reduction of NRF2, and enhancement of NRF2-POMP axis alleviates α-Syn aggregation and neurodegeneration in PD models.

4. Discussion

In this study, we identified a novel role for immunoproteasome in the regulation of α-Syn aggregation and neurodegeneration in PD models (Fig. 6). We further characterized that PLK2, a key phosphokinase of α-Syn Ser129, was a direct target of immunoproteasome. In this case, immunoproteasome dysfunction was sufficient to cause α-Syn Ser129 phosphorylation and aggregation due to the inhibited PLK2 degradation. In response to α-Syn, loss of POMP expression resulting from reduced NRF2 transcription prevented the assembly of immunoproteasome β subunits, thereby suppressing immunoproteasome function. Enhancement of NRF2-POMP axis effectively rescued α-Syn aggregation and neurodegeneration, highlighting the importance of proper assembly for immunoproteasome function in PD pathogenesis.

Various neurodegenerative diseases including PD share a common pathological feature, that is, intracellular protein aggregation such as α-Syn [28,29]. Considerable evidence supports the notion that defective proteasomal degradation is linked to the disruption of cellular proteostasis. The resulting aberrant protein accumulation probably overloads the cellular ability to degrade rendering the dopaminergic neurons susceptible to external and internal stimuli [30]. Recently, we have demonstrated the emerging ideas on the regulation of proteasome homeostasis and the strategies for intensifying proteasomal degradation as a promising approach for PD treatment [10]. Since McNaught and colleagues first reported the impairment of proteasome activities in PD, subsequent studies have verified 26S proteasome dysfunction and its effects on the imbalanced proteostasis [12,31]. Nevertheless, how immunoproteasome function is regulated and the potential role in the neurodegeneration of PD remains unclear. In contrast to 26S proteasome, immunoproteasome has the property of rapid induction and prior assembly, which can degrade substrates independent of ubiquitin and ATP [32]. The function of immunoproteasome extends beyond peptides generation presented by major histocompatibility complex I (MHC I) for $CD8^+$ T cells recognition. Another function relates to the maintenance of protein homeostasis by eliminating ubiquitin-tagged, oxidatively modified or misfolded proteins [15], which supports the implication of immunoproteasome in protein aggregation disorders, such as PD. The present study extended the previous findings and demonstrated that immunoproteasome β1i, β2i, β5i expression and proteolytic activities were remarkedly down-regulated upon exposure to α-Syn, indicating the involvement of immunoproteasome in PD pathogenesis.

Among the numerous posttranslational modifications of α-Syn, a growing interest has focused on Ser129 phosphorylation and its possible role in α-Syn-induced neurodegeneration [6]. To date, the questions about how Ser129 phosphorylation modulates the biological function of α-Syn and whether α-Syn Ser129 phosphorylation promotes or inhibits its aggregation remain controversial. Previous studies have reported that α-Syn Ser129 phosphorylation exhibits an increased binding affinities to metal ions (Cu^{2+}, Pb^{2+}, and Fe^{2+}), which might in turn affect α-Syn aggregation properties [33]. Furthermore, iron overload induces the elevated α-Syn Ser129 phosphorylation, which is largely responsible for the increased protein levels of α-Syn [34]. PLK2 is the kinase for α-Syn phosphorylation at Ser129. In brains of PD patients, increased PLK2 expression is accompanied by the elevated Ser129 phosphorylation of α-Syn. Oral administration of PLK2 inhibitor leads to the

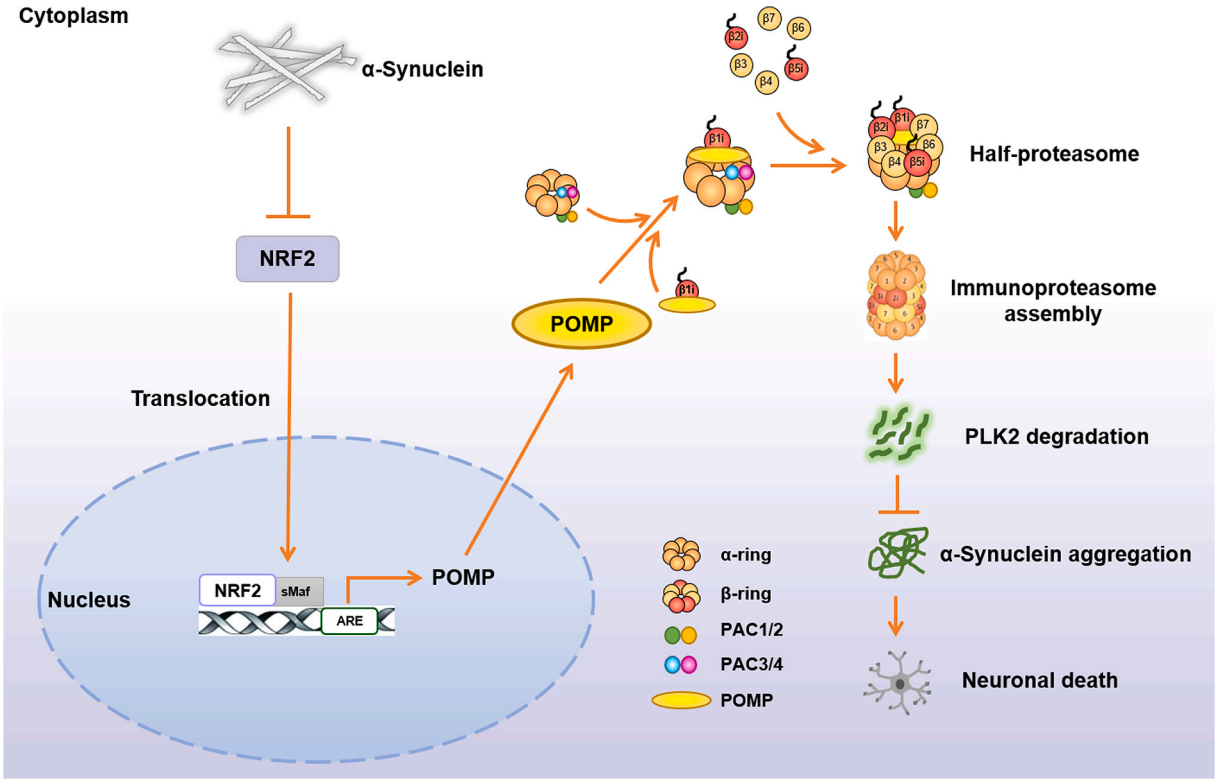

Fig. 6. A schematic diagram underlying the role of immunoproteasome assembly disturbance in α-Syn pathology and neurodegeneration in PD models. Proteasome-assembly chaperone 1/2 (PAC1/2) and PAC3/4 participated in the assembly of core particle α-ring, and then POMP was applied to mediate the assembly of β-ring. In response to α-Syn overexpression, loss of POMP resulting from reduced NRF2 transcription prevented the assembly of immunoproteasome β subunits, thereby suppressing PLK2 degradation, exacerbating α-Syn aggregation and finally leading to neurodegeneration in PD models.

decreased phosphorylation level of α-Syn, which further slows down the loss of dopaminergic neurons [35]. An opposing result has shown that PLK2 overexpression enhances α-Syn clearance via autophagy pathway, implying that PLK2-mediated neuroprotective effect is probably due to the reduction of α-Syn accumulation [36]. Therefore, it would be necessary to understand the exact role of α-Syn Ser129 phosphorylation in its normal function and aggregation in PD. Our data revealed that PLK2 was a previously unrecognized target of immunoproteasome. Not surprisingly, immunoproteasome dysfunction prevented the degradation of PLK2, thereby exacerbating α-Syn Ser129 phosphorylation. Immunoproteasome β5i overexpression could significantly alleviate the accumulation of α-Syn in PD models. PLK2 inhibitor BI2536 treatment could further reduce α-Syn Ser129 phosphorylation and aggregation. These results are in favor of the point that PLK2-mediated α-Syn Ser129 phosphorylation is a harmful factor for α-Syn aggregation and neurotoxicity. Therefore, a proper regulation of immunoproteasome function is beneficial to maintain PLK2 protein stability and protects against α-Syn pathology in PD.

Immunoproteasome homeostasis undergoes dynamic regulation and precise assembly of each subunit is essential to generate adequate immunoproteasome for maintaining normal cellular function. Upon the completion of α-ring assembly, β-subunits subsequently incorporate into the inner surface of α-ring. Immunoproteasome β-subunits, except β3 and β4, are synthesized as precursors with N-terminal propeptides, then undergo cleavage by three catalytic subunits β1i, β2i, and β5i at the completion of β-ring assembly [37]. The only well-described chaperone dedicated to the assembly of β-ring in yeast is ub-mediated proteolysis protein 1 (Ump1), which was first discovered in 1998 [38]. In 2000, a human homologue of Ump1 was characterized and designated as POMP [17]. Although POMP is a key molecular chaperone in the process of immunoproteasome β-ring assembly, the molecular mechanisms regulating POMP expression and the potential role of immunoproteasome assembly disturbance in PD are still not elucidated. Here, we provided several lines of evidence supporting that POMP-mediated immunoproteasome assembly was inhibited in the presence of α-Syn, so as to aggravate the dopaminergic neurons injury in PD models. α-Syn overexpression greatly decreased POMP mRNA and protein levels, restricting the binding of POMP with β5i precursors. As expected, POMP knockdown further exacerbated the decreased β1i, β5i subunits and proteolytic activities induced by α-Syn, favoring the proper β-ring assembly by POMP is indeed necessary to maintain immunoproteasome function.

POMP expression is regulated by the upstream transcription factors NRF2 and NRF3 via a positive feedback loop by binding to POMP promoter [20,26,27]. NRF2 and NRF3, as well as NRF1, belong to the Cap'n'Collar transcription factor family harboring a basic-leucine zipper domain, which binds AREs in the promoter of target genes. As described, NRF1 mediates the gene expression of 26S proteasome subunits in response to proteasome inhibition, which is called "proteasome bounce back response" or "proteasome recovery" [39]. NRF2 directly induces 26S proteasome gene expression under oxidative stress conditions, facilitating the degradation of oxidatively damaged proteins [40]. Interestingly, the promoter of POMP gene also contains ARE sequence, raising the possibility that NRFs can directly modulate the assembly of 20S core particle, besides transcriptionally regulating subunits abundance. Overexpression of POMP by increased NRF2 has been shown to confer bortezomib resistance in myeloma, while their inhibition reversed the resistance [27]. NRF3 directly augments the expression of β-ring assembly chaperone POMP, consequently enhancing the degradation of p53 in a ubiquitin-independent manner [20]. In the present study, we observed that the expression of NRF2, but not NRF1 and NRF3, was decreased upon exposure to α-Syn. In PD, NRF2 is well-known for its neuroprotective effects against oxidative stress and rescuing the loss of dopaminergic neurons [41,42]. Furthermore, α-Syn overexpression aggravates NRF2 deficiency-induced protein aggregation and neuronal death in PD [43]. Our data provided an important clue for NRF2 in immunoproteasome β-ring assembly and enhancement of NRF2-POMP axis significantly rescued the neurodegeneration induced by α-Syn.

Until now, whether or not the number of TH-positive neurons in the SN of A53T α-Syn transgenic mice changes is still in debate. In 2002, Virginia M Lee lab from University of Pennsylvania first generated the transgenic mice overexpressing human mutant A53T α-Syn, and reported that certain cell populations were completely spared including TH-positive neurons in the SN [44]. Later, several studies also demonstrate that the morphology and number of TH-positive neurons in the SN showed no difference between A53T α-Syn transgenic mice and their littermates [45,46]. However, other studies including our previous results have shown opposing results, that is, TH-positive neurons and TH expression were decreased in A53T α-Syn transgenic mice [47,48]. Furthermore, dopamine transporter (DAT) levels seen with ^{11}C-CFT PET in the homozygous A53T mice were dramatically decreased at the age of 6, 9, and 12 months compared to wild type littermates, which might be indicative of nigrostriatal system impairment [49]. This discrepancy might in part be explained by different abundance of α-Syn in A53T α-Syn transgenic mice with different months old. In the present study, we selected the homozygous A53T α-Syn transgenic mice with age varying from 6 to 12 months, which possess high genomic levels, total and insoluble α-Syn expression, and exhibit motor disturbance phenotypes. In addition, the differences in TH-positive neurons measurement protocols and stereological quantification may also generate inconsistent results. Another reason for this discrepancy might arise from the regulation of TH expression by α-Syn, which further induces dopaminergic neurons injury. It is noteworthy that transcription factor Nurr1 can bind with TH gene promoter to increase TH expression, and α-Syn negatively regulates the transcription activity of Nurr1, thus decreasing its downstream gene expression including TH [50,51]. Echoing these results, α-Syn might suppress TH expression through interference with cAMP/PKA-dependent CREB signaling [52]. In this study, a reduction of nigral TH-positive neurons and TH expression was observed in 12-month A53T α-Syn transgenic mice, which could be rescued by enhanced immunoproteasome function in PD models.

In conclusion, the present study reveals a novel role of immunoproteasome dysfunction as a critical contributor in PD pathogenesis. Abnormal immunoproteasome assembly aggravates α-Syn Ser129 phosphorylation and aggregation by preventing PLK2 degradation, thereby leading to the neurodegeneration in PD models. Inhibition of α-Syn accumulation remains a compelling approach for PD modification. Therefore, enhanced immunoproteasome assembly mediated by NRF2-POMP axis might open up new avenues for PD therapeutic development.

Consent for publication

All authors have read the manuscript and indicated consent for publication.

Data availability statement

All data generated or analyzed during this study are included.

Funding

This work was supported by the National Natural Science Foundation of China (31771110, 32171131, 82071429), Shandong Province Natural Science Foundation (ZR2019ZD31, ZR2020MC072, ZR2020QH125), Taishan Scholars Construction Project, and Innovative Research Team of High-Level Local Universities in Shanghai.

Author contributions

MB and HJ designed the research study. MB and XX performed the experiments. YD, QJ and XC analyzed the data. MB wrote the

manuscript and XD commented on it. LZ provided excellent technical assistance. HJ reviewed the manuscript and supervised the project. All authors have read and approved the final version of the manuscript.

Declaration of competing interest

The authors declare that they have no known competing financial interests or personal relationships that could have appeared to influence the work reported in this paper.

Abbreviations

α-Syn	α-synuclein
AAV	adeno-associated virus
ARE	antioxidant response element
DAT	dopamine transporter
DEGs	differentially expressed genes
DMSO	dimethyl sulfoxide
IFN-γ	interferon-γ
MTT	3-(4,5-dimethyl-2-thiazolyl)-2,5-diphenyl-2-H-tetrazolium bromide
MHC I	major histocompatibility complex I
NRF2	nuclear factor erythroid 2-like 2
PAC	proteasome-assembly chaperone
PD	Parkinson's disease
PFA	paraformaldehyde
PLK2	polo-like kinase 2
POMP	proteasome maturation protein
SN	substantia nigra
ThT	thioflavin T
TH	tyrosine hydroxylase

Appendix A. Supplementary data

Supplementary data to this article can be found online at https://doi.org/10.1016/j.redox.2021.102167.

References

[1] B.R. Bloem, M.S. Okun, C. Klein, Parkinson's disease, Lancet 397 (2021) 2284–2303.
[2] A.S. Harms, S.A. Ferreira, M. Romero-Ramos, Periphery and brain, innate and adaptive immunity in Parkinson's disease, Acta Neuropathol. 141 (2021) 527–545.
[3] G. Runwal, R.H. Edwards, The membrane interactions of synuclein: physiology and pathology, Annu. Rev. Pathol. 16 (2021) 465–485.
[4] M.G. Spillantini, M.L. Schmidt, V.M. Lee, J.Q. Trojanowski, R. Jakes, M. Goedert, Alpha-synuclein in Lewy bodies, Nature 388 (1997) 839–840.
[5] J.P. Anderson, D.E. Walker, J.M. Goldstein, R. de Laat, K. Banducci, R. J. Caccavello, R. Barbour, J. Huang, K. Kling, M. Lee, L. Diep, P.S. Keim, X. Shen, T. Chataway, M.G. Schlossmacher, P. Seubert, D. Schenk, S. Sinha, W.P. Gai, T. J. Chilcote, Phosphorylation of Ser-129 is the dominant pathological modification of alpha-synuclein in familial and sporadic Lewy body disease, J. Biol. Chem. 281 (2006) 29739–29752.
[6] A. Oueslati, Implication of alpha-synuclein phosphorylation at S129 in synucleinopathies: what have we learned in the last decade? J. Parkinsons Dis. 6 (2016) 39–51.
[7] K.J. Inglis, D. Chereau, E.F. Brigham, S.S. Chiou, S. Schobel, N.L. Frigon, M. Yu, R. J. Caccavello, S. Nelson, R. Motter, S. Wright, D. Chian, P. Santiago, F. Soriano, C. Ramos, K. Powell, J.M. Goldstein, M. Babcock, T. Yednock, F. Bard, G.S. Basi, H. Sham, T.J. Chilcote, L. McConlogue, I. Griswold-Prenner, J.P. Anderson, Polo-like kinase 2 (PLK2) phosphorylates alpha-synuclein at serine 129 in central nervous system, J. Biol. Chem. 284 (2009) 2598–2602.
[8] C.T. Hong, K.Y. Chen, W. Wang, J.Y. Chiu, D. Wu, T.Y. Chao, C.J. Hu, K.D. Chau, O. A. Bamodu, Insulin resistance promotes Parkinson's disease through aberrant expression of alpha-synuclein, mitochondrial dysfunction, and deregulation of the polo-like kinase 2 signaling, Cells 9 (2020) 740.
[9] M.S. Hipp, P. Kasturi, F.U. Hartl, The proteostasis network and its decline in ageing, Nat. Rev. Mol. Cell Biol. 20 (2019) 421–435.
[10] M. Bi, X. Du, Q. Jiao, X. Chen, H. Jiang, Expanding the role of proteasome homeostasis in Parkinson's disease: beyond protein breakdown, Cell Death Dis. 12 (2021) 154.
[11] B. Boland, W.H. Yu, O. Corti, B. Mollereau, A. Henriques, E. Bezard, G.M. Pastores, D.C. Rubinsztein, R.A. Nixon, M.R. Duchen, G.R. Mallucci, G. Kroemer, B. Levine, E.L. Eskelinen, F. Mochel, M. Spedding, C. Louis, O.R. Martin, M.J. Millan, Promoting the clearance of neurotoxic proteins in neurodegenerative disorders of ageing, Nat. Rev. Drug Discov. 17 (2018) 660–688.
[12] K.S. McNaught, P. Jenner, Proteasomal function is impaired in substantia nigra in Parkinson's disease, Neurosci. Lett. 297 (2001) 191–194.
[13] H.K. Johnston-Carey, L.C. Pomatto, K.J. Davies, The Immunoproteasome in oxidative stress, aging, and disease, Crit. Rev. Biochem. Mol. Biol. 51 (2015) 268–281.
[14] B.L. Zerfas, M.E. Maresh, D.J. Trader, The immunoproteasome: an emerging target in cancer and autoimmune and neurological disorders, J. Med. Chem. 63 (2020) 1841–1858.
[15] U. Seifert, L.P. Bialy, F. Ebstein, D. Bech-Otschir, A. Voigt, F. Schroter, T. Prozorovski, N. Lange, J. Steffen, M. Rieger, U. Kuckelkorn, O. Aktas, P. M. Kloetzel, E. Kruger, Immunoproteasomes preserve protein homeostasis upon interferon-induced oxidative stress, Cell 142 (2010) 613–624.
[16] A. Rousseau, A. Bertolotti, Regulation of proteasome assembly and activity in health and disease, Nat. Rev. Mol. Cell Biol. 19 (2018) 697–712.
[17] E. Witt, D. Zantopf, M. Schmidt, R. Kraft, P.M. Kloetzel, E. Kruger, Characterisation of the newly identified human Ump1 homologue POMP and analysis of LMP7(beta 5i) incorporation into 20 S proteasomes, J. Mol. Biol. 301 (2000) 1–9.
[18] A.J. Marques, R. Palanimurugan, A.C. Matias, P.C. Ramos, R.J. Dohmen, Catalytic mechanism and assembly of the proteasome, Chem. Rev. 109 (2009) 1509–1536.
[19] S. Heink, D. Ludwig, P.M. Kloetzel, E. Kruger, IFN-gamma-induced immune adaptation of the proteasome system is an accelerated and transient response, Proc. Natl. Acad. Sci. U. S. A. 102 (2005) 9241–9246.
[20] A. Kobayashi, T. Waku, New addiction to the NRF2-related factor NRF3 in cancer cells: ubiquitin-independent proteolysis through the 20S proteasome, Cancer Sci. 111 (2020) 6–14.
[21] Z. Zhang, X. Du, H. Xu, J. Xie, H. Jiang, Lesion of medullary catecholaminergic neurons is associated with cardiovascular dysfunction in rotenone-induced Parkinson's disease rats, Eur. J. Neurosci. 42 (2015) 2346–2355.
[22] M. Bi, X. Du, Q. Jiao, Z. Liu, H. Jiang, Alpha-synuclein regulates iron homeostasis via preventing parkin-mediated DMT1 ubiquitylation in Parkinson's disease models, ACS Chem. Neurosci. 11 (2020) 1682–1691.
[23] J.A. Nathan, V. Spinnenhirn, G. Schmidtke, M. Basler, M. Groettrup, A.L. Goldberg, Immuno- and constitutive proteasomes do not differ in their abilities to degrade ubiquitinated proteins, Cell 152 (2013) 1184–1194.
[24] F. Cao, X. Xia, Y. Fan, Q. Liu, J. Song, Q. Zhang, Y. Guo, S. Yao, Knocking down of Polo-like kinase 2 inhibits cell proliferation and induced cell apoptosis in human glioma cells, Life Sci. 270 (2021) 119084.
[25] Y.S. Yun, K.H. Kim, B. Tschida, Z. Sachs, K.E. Noble-Orcutt, B.S. Moriarity, T. Ai, R. Ding, J. Williams, L. Chen, D. Largaespada, D.H. Kim, mTORC1 coordinates protein synthesis and immunoproteasome formation via PRAS40 to prevent accumulation of protein stress, Mol Cell 61 (2016) 625–639.
[26] T. Waku, N. Nakamura, M. Koji, H. Watanabe, H. Katoh, C. Tatsumi, N. Tamura, A. Hatanaka, S. Hirose, H. Katayama, M. Tani, Y. Kubo, J. Hamazaki, T. Hamakubo, A. Watanabe, S. Murata, A. Kobayashi, NRF3-POMP-20S proteasome assembly Axis promotes cancer development via ubiquitin-independent proteolysis of p53 and retinoblastoma protein, Mol. Cell Biol. 40 (2020) e00597-19.
[27] B. Li, J. Fu, P. Chen, X. Ge, Y. Li, I. Kuiatse, H. Wang, X. Zhang, R.Z. Orlowski, The nuclear factor (Erythroid-derived 2)-like 2 and proteasome maturation protein Axis mediate bortezomib resistance in multiple myeloma, J. Biol. Chem. 290 (2015) 29854–29868.
[28] A. Tarutani, M. Hasegawa, Prion-like propagation of alpha-synuclein in neurodegenerative diseases, Prog Mol Biol Transl Sci 168 (2019) 323–348.
[29] Y.J. Guo, H. Xiong, K. Chen, J.J. Zou, P. Lei, Brain regions susceptible to alpha-synuclein spreading, Mol. Psychiatr. (2021).
[30] T.A. Thibaudeau, R.T. Anderson, D.M. Smith, A common mechanism of proteasome impairment by neurodegenerative disease-associated oligomers, Nat. Commun. 9 (2018) 1097.
[31] H.J. Rideout, K.E. Larsen, D. Sulzer, L. Stefanis, Proteasomal inhibition leads to formation of ubiquitin/alpha-synuclein-immunoreactive inclusions in PC12 cells, J. Neurochem. 78 (2001) 899–908.
[32] S. Murata, Y. Takahama, M. Kasahara, K. Tanaka, The immunoproteasome and thymoproteasome: functions, evolution and human disease, Nat. Immunol. 19 (2018) 923–931.
[33] Y. Lu, M. Prudent, B. Fauvet, H.A. Lashuel, H.H. Girault, Phosphorylation of alpha-Synuclein at Y125 and S129 alters its metal binding properties: implications for understanding the role of alpha-Synuclein in the pathogenesis of Parkinson's Disease and related disorders, ACS Chem. Neurosci. 2 (2011) 667–675.
[34] R. Wang, Y. Wang, L. Qu, B. Chen, H. Jiang, N. Song, J. Xie, Iron-induced oxidative stress contributes to alpha-synuclein phosphorylation and up-regulation via polo-like kinase 2 and casein kinase 2, Neurochem. Int. 125 (2019) 127–135.
[35] D.L. Aubele, R.K. Hom, M. Adler, R.A. Galemmo Jr., S. Bowers, A.P. Truong, H. Pan, P. Beroza, R.J. Neitz, N. Yao, M. Lin, G. Tonn, H. Zhang, M.P. Bova, Z. Ren, D. Tam, L. Ruslim, J. Baker, L. Diep, K. Fitzgerald, J. Hoffman, R. Motter, D. Fauss, P. Tanaka, M. Dappen, J. Jagodzinski, W. Chan, A.W. Konradi, L. Latimer, Y.L. Zhu, H.L. Sham, J.P. Anderson, M. Bergeron, D.R. Artis, Selective and brain-permeable polo-like kinase-2 (Plk-2) inhibitors that reduce alpha-synuclein phosphorylation in rat brain, ChemMedChem 8 (2013) 1295–1313.
[36] A. Oueslati, B.L. Schneider, P. Aebischer, H.A. Lashuel, Polo-like kinase 2 regulates selective autophagic alpha-synuclein clearance and suppresses its toxicity in vivo, Proc. Natl. Acad. Sci. U. S. A. 110 (2013) E3945–E3954.
[37] R.J. Tomko Jr., M. Hochstrasser, Molecular architecture and assembly of the eukaryotic proteasome, Annu. Rev. Biochem. 82 (2013) 415–445.

[38] P.C. Ramos, J. Hockendorff, E.S. Johnson, A. Varshavsky, R.J. Dohmen, Ump1p is required for proper maturation of the 20S proteasome and becomes its substrate upon completion of the assembly, Cell 92 (1998) 489–499.
[39] S.K. Radhakrishnan, C.S. Lee, P. Young, A. Beskow, J.Y. Chan, R.J. Deshaies, Transcription factor Nrf1 mediates the proteasome recovery pathway after proteasome inhibition in mammalian cells, Mol Cell 38 (2010) 17–28.
[40] A.M. Pickering, R.A. Linder, H. Zhang, H.J. Forman, K.J. Davies, Nrf2-dependent induction of proteasome and Pa28alphabeta regulator are required for adaptation to oxidative stress, J. Biol. Chem. 287 (2012) 10021–10031.
[41] C. Bento-Pereira, A.T. Dinkova-Kostova, Activation of transcription factor Nrf2 to counteract mitochondrial dysfunction in Parkinson's disease, Med. Res. Rev. 41 (2021) 785–802.
[42] L. Fao, S.I. Mota, A.C. Rego, Shaping the Nrf2-ARE-related pathways in Alzheimer's and Parkinson's diseases, Ageing Res. Rev. 54 (2019) 100942.
[43] I. Lastres-Becker, A. Ulusoy, N.G. Innamorato, G. Sahin, A. Rabano, D. Kirik, A. Cuadrado, alpha-Synuclein expression and Nrf2 deficiency cooperate to aggravate protein aggregation, neuronal death and inflammation in early-stage Parkinson's disease, Hum. Mol. Genet. 21 (2012) 3173–3192.
[44] B.I. Giasson, J.E. Duda, S.M. Quinn, B. Zhang, J.Q. Trojanowski, V.M. Lee, Neuronal alpha-synucleinopathy with severe movement disorder in mice expressing A53T human alpha-synuclein, Neuron 34 (2002) 521–533.
[45] S. Zhang, Q. Xiao, W. Le, Olfactory dysfunction and neurotransmitter disturbance in olfactory bulb of transgenic mice expressing human A53T mutant alpha-synuclein, PLoS One 10 (2015), e0119928.
[46] E. Sotiriou, D.K. Vassilatis, M. Vila, L. Stefanis, Selective noradrenergic vulnerability in alpha-synuclein transgenic mice, Neurobiol. Aging 31 (2010) 2103–2114.
[47] S.B. Rangasamy, S. Dasarathi, P. Pahan, M. Jana, K. Pahan, Low-Dose aspirin upregulates tyrosine hydroxylase and increases dopamine production in dopaminergic neurons: implications for Parkinson's disease, J. Neuroimmune Pharmacol. 14 (2019) 173–187.
[48] L. Jiao, X. Du, F. Jia, Y. Li, D. Zhu, T. Tang, Q. Jiao, H. Jiang, Early low-dose ghrelin intervention via miniosmotic pumps could protect against the progressive dopaminergic neuron loss in Parkinson's disease mice, Neurobiol. Aging 101 (2021) 70–78.
[49] W. Wang, N. Song, F. Jia, T. Tang, W. Bao, C. Zuo, J. Xie, H. Jiang, Genomic DNA levels of mutant alpha-synuclein correlate with non-motor symptoms in an A53T Parkinson's disease mouse model, Neurochem. Int. 114 (2018) 71–79.
[50] C. Jia, H. Qi, C. Cheng, X. Wu, Z. Yang, H. Cai, S. Chen, W. Le, Alpha-synuclein negatively regulates Nurr1 expression through NF-kappaB-Related mechanism, Front. Mol. Neurosci. 13 (2020) 64.
[51] J. Zou, Z. Chen, X. Wei, Z. Chen, Y. Fu, X. Yang, D. Chen, R. Wang, P. Jenner, J. H. Lu, M. Li, Z. Zhang, B. Tang, K. Jin, Q. Wang, Cystatin C as a potential therapeutic mediator against Parkinson's disease via VEGF-induced angiogenesis and enhanced neuronal autophagy in neurovascular units, Cell Death Dis. 8 (2017), e2854.
[52] S.S. Kim, K.R. Moon, H.J. Choi, Interference of alpha-synuclein with cAMP/PKA-dependent CREB signaling for tyrosine hydroxylase gene expression in SK-N-BE(2) C cells, Arch Pharm. Res. (Seoul) 34 (2011) 837–845.